The Temperature-Dependence of Charge Carrier Concentrations in Low-Dimensional Metals: A Breathing Band Gap Model

M. T. Green,* V. Robert, and J. K. Burdett

Department of Chemistry and James Franck Institute, The University of Chicago, 5735 South Ellis Avenue, Chicago, Illinois 60637

Received: August 1, 1997; In Final Form: September 22, 1997[⊗]

Within the framework of a very simple model of vibronic origin, we investigate the temperature-dependent concentration of charge carriers in the conduction band of a low-dimensional metallic system. The participation of phonons is pointed out by concentrating on the oscillations of nuclei as a function of temperature. On the basis of the assumption that conductivity can be directly related to the number of charge carriers in the conduction band, our model predicts a decreasing conductivity with temperature, in good agreement with experimental observations. For high temperatures we find the number of carriers to vary as $\boldsymbol{T}^{-1.04}$. Using band structure calculations, we therefore obtain original insight into electronic scattering in solids.

I. Introduction

If one is interested in describing electron transport phenomena in solids, electron−phonon interactions have to be taken into consideration. A prime example of this can be seen in the temperature-dependent resistivity of metals. Indeed, while one expects the number of charge carriers and, as a result, the conductivity to increase with temperature, it is well-established that resistivity in metals, resulting from electron−phonon scattering, increases with temperature. To address this issue, many phenomenological models have been suggested in the literature. In molecular systems, electron localization resulting from the vibronic coupling of ground and excited states has been studied extensively and is now well-understood.[1] Öpik and Pryce[2] have shown how to analytically determine the adiabatic potential and, within the framework of a three-parameter phenomenological model, the mixing of electronic terms resulting in the so-called Jahn−Teller and pseudo Jahn−Teller effects.[3] This approach has been extensively used to describe electron localization in biological mixed-valence clusters.[4] In these cases, modulation of either charge transfer or on-site energy with vibronic interactions were emphasized and led to the original physical understanding of charge transport phenomena.[5,6]

As far as extended systems are concerned, efforts have been mainly restricted to phenomenological electron−phonon coupling models.[7,8] Many studies have been carried out in order to make contact with important properties of crystal lattices such as specific heat, conductivity, solitons,[9] and magnetoresistance.[10] The usual way to estimate macroscopic quantities associated with these properties is to solve Boltzmann's equation which describes microscopic motions by means of a statistical distribution function. In doing so, the "relaxation time approximation" is frequently assumed to depict scattering from the lattice.[11] While these relaxation time models have been very successful in explaining numerous phenomena associated with electron transport, they offer very little in the way of chemical intuition. It is for this reason that we attempted to develop a model of scattering which takes into account the variation of electronic energy levels with nuclear motion. We felt that if one could observe the change in the number of charge carriers as a function of a temperature-dependent vibrating band gap, a clearer and more intuitive feel for what is meant by electron−phonon scattering might result. We therefore decided to investigate the effect of temperature on a one-dimensional chain. To do this we assumed harmonic nuclear motion, and that the gap, which opened as a result of this motion, could be related to the change in overlap between two adjacent atomic centers. The number of charge carriers in the conduction band of such a system results from a competition between the thermal population of electronic states and the temperature driven band gap. The former effect pushes electrons up into the conduction band whereas the latter effectively reduces its population. Thus, by assuming a direct correlation with the number of charge carriers a connection to conductivity can be made.

We now provide details of the original model which we have used in order to assess the role of these two temperature-dependent effects.

II. Description of the Breathing Band Gap Model

Band structure calculations are well-adapted to take into consideration the real chemical and geometrical properties of solids. It has been shown that such theoretical approaches based on either the local density or generalized gradient approximations provided an effective way to accurately estimate one-electron and many-body terms.[12] Full potential linear augmented plane wave (LAPW) calculations using these approaches have thus been able to reproduce structural parameters of solids with high precision.[13] Keeping this in mind, we first concentrate on a one-dimensional linear chain made from orbitals of a given type χ with lattice parameter a. Let us define $\chi(r - R_p)$, $R_p = pa$ as the atomic orbital located on the atom of the pth unit cell. One can then easily generate the symmetry-adapted linear combinations $\phi(r,k)$ as

$$\phi(r,k) = \frac{1}{\sqrt{N}} \sum_p e^{ikR_p} \chi(r - R_p) \qquad (1)$$

where $\sqrt{N}$ is the normalizing factor.[14] In (1) overlaps between atomic orbital wave functions are neglected according to the traditional Hückel approximation. With only nearest neighbor-interactions along the chain, a general expression for the energy is known to be $e(k) = \alpha + 2\beta \cos(ka)$, where α and β are often called Coulomb and resonance integrals, respectively.

* To whom correspondence should be addressed. E-mail: green@rainbow.uchicago.edu. Fax: (773) 702 0805.

⊗ Abstract published in *Advance ACS Abstracts,* November 15, 1997.

S1089-5647(97)02507-8 CCC: $14.00

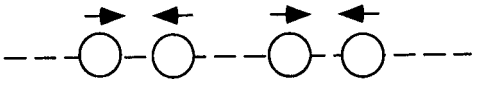

Figure 1. Schematic representation of ω_o − mode. Atoms are shown in some displaced positions.

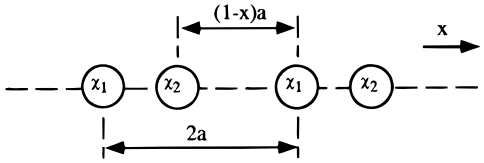

Figure 2. Bond alternation structure of studied one-dimensional system. $x < 0$ on this picture.

If one is interested in looking at the coupling between electronic and nuclear motions, some attention should be paid to the classical phonon dispersion curve. Consider the elastic vibration of a our model crystal. The angular frequency of an elastic wave in terms of the wavevector may be written as

$$\omega = \omega_o \left|\sin\left(\frac{ka}{2}\right)\right| \tag{2}$$

where ω_o^2 is proportional to the nearest-neighbor elastic interaction.[11] At the Brillouin zone boundaries $k_{max} = \pm\pi/a$, the solution is a standing wave of angular frequency ω_o. Since alternate atoms oscillate with opposite phase (Figure 1), one can assume that the excitations of such a mode, which we will refer to as the ω_o − mode, will bring about the largest change in the band structure. This is Peierls's theorem.[15] To study this mode and its effect upon the conductivity, it is necessary to double the cell. This procedure is straightforward and leads to the usual "folding-back"[16] of the dispersion curve. Thus the energy levels of the new cell are

$$e_{\pm}(k) = \alpha \pm 2\beta \cos(ka) \tag{3}$$

In (3), however, k runs from 0 to $\pi/2a$ and no confusion should be made with the previous relation where k ran from 0 to π/a.

We wish to examine the effect of vibrations upon the energy bands given in (3). This problem is closely related to the bond alternated band calculations of polyacetylene.[14] Using these as a guide line we first locate χ_1 and χ_2 on the left- and right-hand side atoms of any given unit cell. If xa, $-1 < x < 1$, characterizes bond alternation (Figure 2), Bloch's functions may be written as

$$\phi_1(r,k) = \frac{1}{\sqrt{N}}\sum_p e^{i2pka}\chi_1(r - 2pa)$$

$$\phi_2(r,k) = \frac{1}{\sqrt{N}}\sum_p e^{i(2p+1+x)ka}\chi_1(r - (2p + 1 + x)a) \tag{4}$$

We can model bond alternation by then making

$$\langle\chi_1(r - 2pa)|\tilde{\boldsymbol{H}}|\chi_2(r - (2p + 1 - x)a)\rangle = \beta - \lambda(x)$$

$$\langle\chi_2(r - (2p + 1 + x)a)|\tilde{\boldsymbol{H}}|\chi_1(r - 2pa)\rangle = \beta + \lambda(x) \tag{5}$$

where $\lambda(x)$ accounts for vibronic interactions. Solution of the secular determinant leads to

$$e_{\pm}(k) = \alpha \pm 2\beta\left\{\cos^2(ka) + \frac{\lambda^2(x)}{\beta^2}\sin^2(ka)\right\}^{1/2} \tag{6}$$

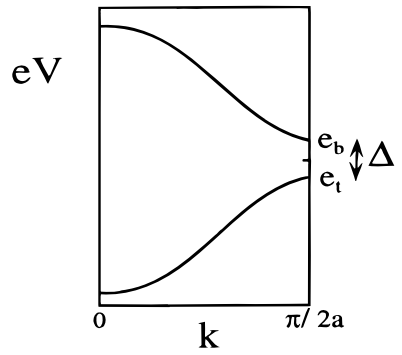

Figure 3. Dispersion behavior with account of vibronic coupling. e_t and e_b stand for the top and the bottom of valence and conduction bands, respectively.

Unless $\lambda(x) = 0$, the band structure defined by (6) reflects a splitting of the degeneracy at the zone edge (Figure 3) characterized by $\Delta = 2|\lambda(x)| = e_b - e_t$, where e_t and e_b stand for the top and the bottom of valence and conduction bands, respectively.

We now wish to obtain an expression for λ, the vibronic interaction energy, as a function of temperature T. To do so we assume that x, which is related to the vibrational amplitude, is harmonic in motion, and that λ is proportional to the root-mean-square displacement of this motion. To obtain the band structures for each nuclear displacement we further assume that the electrons move much faster than the nuclei. If this is the case, the so-called adiabatic approximation is valid as long as the energy spectrum does not contain any degenerate or quasi-degenerate states. Our use of this approximation here relies on the fact that in this system degeneracy may occur only at the zone edge. As a result, we can obtain the bands by solving a secular determinant for each given value of the parameter x. Since in what follows we will be interested in time average effects we should also express x, and therefore λ, as a function of time. Thus we would expect $\lambda(t)$ to have the following form:

$$\lambda(t) = \kappa a\beta[\{\langle x^2\rangle_T\}^{1/2} - \{\langle x^2\rangle_{T=0}\}^{1/2}]\sin(\omega_o t) \tag{7}$$

where κ is a proportionality parameter associated with the change in nearest-neighbor overlap, β is the resonance integral, $\langle x^2\rangle_T$ is the mean-square value of the displacement of a harmonic oscillator at temperature T, and ω_o is the frequency of the phonon mode. In (7) we have subtracted out the root-mean-square of the zero point motion in order to remove variations in the nearest neighbor interaction at $T = 0$ K. This gives a reference state with which changes may be compared. The value of the mean-square nuclear displacements $\langle x^2\rangle_T$ are obtained by thermally populating the levels of a harmonic oscillator of angular frequency ω_o and mass μ. It can be easily shown that

$$\langle x^2\rangle_T = \frac{\hbar}{\mu\omega_o a^2}\coth\left(\frac{\tau\hbar\omega_o}{2}\right) = \langle x^2\rangle_{T=0}\coth\left(\frac{\tau\hbar\omega_o}{2}\right) \tag{8}$$

where $\tau = 1/k_B T$, k_B stands for Boltzmann's constant.[17] For a given temperature, the maximum nuclear displacements will of course be larger than the root of the quantity given by (8), and as a result one might expect that the use of $\langle x^2\rangle_T$ in (7) would lead to values of λ smaller than those obtained from an interaction varying linearly with nuclear displacement. However, if we assume that these distances may be related through a quantity which can be absorbed into the coupling constant κ, it is possible to view (7) as an interaction in which the linear dependence has been transformed from the nuclear displacement

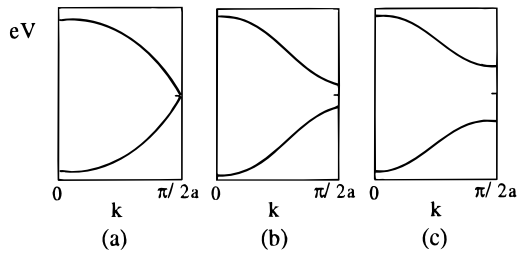

Figure 4. Breathing band structure as a function of time: (a) $\omega_o t = 0$; (b) $\omega_o t = \pi/4$; (c) $\omega_o t = \pi/2$. Other parameters used were $\alpha = -5.5$ eV, $\beta = -2.2$ eV, and $\kappa = 0.7$ (bohr)$^{-1}$.

to the root-mean-square of this quantity. The generation of a secular determinant for each time t leads to

$$e_{\pm}(k) = \alpha \pm 2\beta\{\cos^2(ka) + (\kappa a)^2[\{\langle x^2\rangle_T\}^{1/2} - \{\hbar/\mu\omega_o a^2\}^{1/2}]^2 \sin^2(\omega_o t)\sin^2(ka)\}^{1/2} \quad (9)$$

Figure 4 shows the band structure evolution for a given set of α, β, and κ. One can notice the breathing band gap phenomenon associated with ω_o − phonons. In what follows we attempt to connect changes in electrical conductivity with such a behavior. We will show how thermal population competes with the oscillating band gap Δ and trace the net concentration of intrinsic carriers.

III. Charge Carrier Calculations

Up to this point, we have developed a model that makes it possible to estimate the band structure of any linear chain as a function of time and temperature. We are now interested in tracing the number of charge carriers in the conduction band resulting from the occupation of these states by the Fermi−Dirac distribution (10).

$$f(\epsilon) = \frac{1}{e^{\tau(\epsilon-\epsilon_F)} + 1} \quad (10)$$

The correct location of the chemical potential ϵ_F is determined so as to maintain the number of electrons the same for all temperatures. Since we are dealing with a dynamic situation, the quantity we seek is an average of the number of charge carriers over a period of vibration, $t_o = 2\pi/\omega_o$. The distribution (10), which is used to calculate this average, however, is an equilibrium distribution, and as a result, some care must be taken in its use. If electron−hole recombination rates are fast on the time scale of vibrations then the use of the equilibrium distribution (10) at each instant in time is valid, and the average number of charge carriers is calculated for each temperature as follows:

$$\sigma(T) = \langle 2\int_{e_b}^{\infty} f(\epsilon)g(\epsilon)\,d\epsilon\rangle \quad (11a)$$

where $g(\epsilon)$ is the density of states for energy ϵ. If, on the other hand, the system equilibrates slowly on the time scale of vibrations, electron−hole pairs will not recombine for many vibrational periods. For this case, it is improper to use (10) in the manner discussed above. Here it is best to define a time averaged electronic density of states, and to then populate this with the Fermi−Dirac distribution. In this situation the average number of carriers is

$$\sigma(T) = 2\int_{e_b}^{\infty} f(\epsilon)\langle g(\epsilon)\rangle_t\,d\epsilon \quad (11b)$$

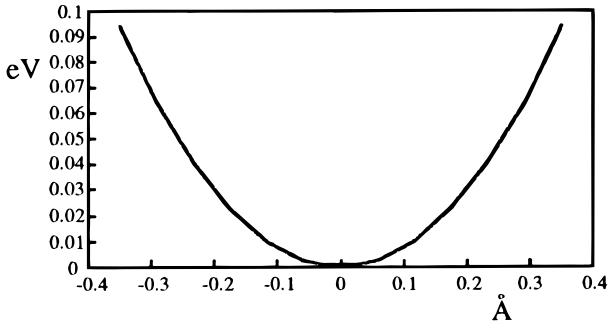

Figure 5. Adiabatic potential surface exhibiting energy as a function of Q_{111} vibrational coordinate. ω_0 is readily accessible out of this plot.

We have used these complementary methods to study the thermal dependence of charge carrier concentrations within the conduction band.

It is tempting to assume that the electrical conductivity is basically controlled by the population of levels with energy higher than e_b. Raising the temperature should obviously increase this population. On the other hand, it should also open a wider gap resulting in an increasing e_b value. Therefore, one can expect a competition between these two effects mirroring the temperature-dependent conductivity in metals. Our model primarily relies on this chemically intuitive picture, the results of which we will examine in the next section.

IV. Results and Discussion

To fill out the framework of our model, we chose to investigate a linear chain of lithium atoms. Using the LAPW method we performed calculations on a bcc Li lattice to obtain information about the adiabatic potential surface.[13] Details concerning these calculations are given in the Appendix. Since the system which we are modeling and the system upon which the calculations were performed are of different dimensionalities, we should point out here that the purpose of these calculations was to obtain a reasonable value for the angular frequency ω_o. We therefore concentrated on the symmetry-breaking 111-distortion which is equivalent to the ω_o − mode of the linear chain. The potential energy of any system can be expanded in a power series over normal coordinates $\{Q_\Gamma\}$ as

$$V(r,\{Q_\Gamma\}) = V(r,\{Q_\Gamma^0\}) + {}^1/_2\sum_{Q_\Gamma,Q_{\Gamma'}} \frac{\partial^2 V}{\partial Q_\Gamma \partial Q_{\Gamma'}}(Q_\Gamma - Q_\Gamma^0)(Q_{\Gamma'} - Q_{\Gamma'}^0) + \ldots \quad (12)$$

where $\{Q_\Gamma^0\}$ refer to equilibrium geometry. Thus, assuming that the system is most sensitive to vibration along the 111-direction, we may approximate (12) as

$$V(r,\{Q_\Gamma\}) \approx V(r,\{Q_\Gamma^0\}) + {}^1/_2\Lambda(Q_{111} - Q_{111}^0)^2 + \ldots \quad (13)$$

Figure 5 displays the potential shape which does not exhibit much anharmonicity. Note that we have chosen our energy origin at $Q_{111} = Q_{111}^0$. Upon the basis of this approximation, a value of 6.50×10^{13} s^{-1} was calculated for ω_o directly accessible from (14) where m stands for the atomic mass. One should notice that the harmonic oscillator's mass μ and m are not equal. However, it can be easily shown that $\mu = m/2$ (reduced mass relationship).

$$\omega_o = \left(\frac{2\Lambda}{m}\right)^{1/2} \quad (14)$$

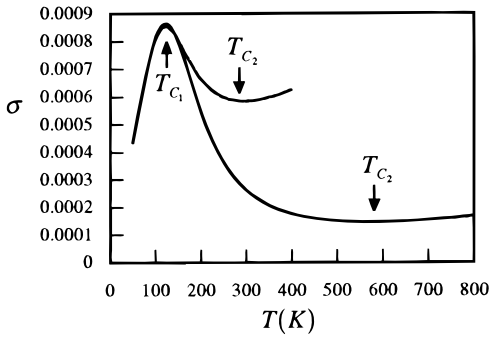

Figure 6. Number of charge carriers in the conduction band as a function of temperature. Upper curve corresponds to the use of the actual gap, i.e. (11a). Bottom curve corresponds to the use of the time averaged band gap, i.e. (11b).

As for the other variables in (7), α and β were estimated from extended Hückel parameters, while κ, the change in overlap of two Slater type orbitals, was approximated by the Slater coefficient.[18] These values are consistent with the ω_o value estimation, and were used to assess the validity of our model.

Numerical calculations for (11a,b) are shown in Figure 6 where each curve is divided into three areas by the temperatures T_{C_1} and T_{C_2}. While these curves have the same general features, their values differ markedly above T_{C_1}. Below this temperature the curves are almost identical, and this indistinguishability results from the small difference between the time averaged and actual band gaps within this region. This difference increases with temperature, and as it does the results of two methods deviate. The actual shape of the curves in the low-temperature region reflects that at $T = 0$ K there can be no population of the conduction band. Thus, as the temperature rises initially, the number of carriers can only increase. As the temperature continues to grow however, so do the vibrational amplitudes of the nuclear centers. The band gap created by this motion directly competes with temperature in order to determine the population of the conduction band. In the region between T_{C_1} and T_{C_2} the vibrations have won out and the number of charge carriers decreases with increasing temperature. This looks like the behavior one expects for conduction in metallic systems. To further the connection between the number of charge carriers in the conduction band and electrical conductivity we fit the data with a single-valued polynomial T^{ξ}. Use of (11a) gives a value of $\xi = -0.58$ ($r^2 = -0.99$) in the region $T = 130-260$ K, while (11b) gives $\xi = -1.5$ ($r^2 = -0.98$). Since the two methods employed lie at the extremes of electron−hole recombination rates, one might imagine that a more accurate description would be intermediate to these values, but recombination rates on the order of nanoseconds in Ge and Si suggest that the description, at least in these materials, best lies with (11b). Examination of Figure 6 shows that the use of (11b) raises T_{C_2} by almost 300 K over that found using (11a). Applying a similar fit to this region results in $\xi = -1.04$ ($r^2 = -0.98$) for $T = 310-510$ K. This can be compared with the value of $\xi_{e-ph} = -1.0$ obtained from electron−phonon collision theory for high-temperature conductivity.[11] Thus it would appear that in this region there is a nice correlation between the number of charge carriers and electrical conductivity. However, there are certainly other factors involved.

The highest temperature regions of Figure 6 (above T_{C_2}) are a bit confusing since one expects conductivity in metallic systems to be a monotonically decreasing function of temperature, but as can clearly be seen the number of charge carriers increases. As a result, we must reexamine our model and assess its validity in this region. Looking at (8) for high temperatures one finds

$$\langle x^2 \rangle_T \approx \frac{2k_B T}{\mu \omega^2{}_o a^2} \tag{15}$$

Also at high temperatures the Fermi distribution for the maximum gap Δ_{max} reduces to Boltzmann's factor $e^{-\Delta_{max}/k_B T}$. This when combined with (15) should go as $e^{-(\Theta/T)^{1/2}}$ where $\Theta = 8\kappa^2\beta^2/k_B\mu\omega^2{}_o a^2$. This, however, is just the well-established behavior of intrinsic carriers in semiconductors given a band gap which varies as $\sqrt{T}$. So we see that in this region the temperature always outruns the gap. Thus the number of charge carriers increases, and our model no longer represents a metallic system. An examination of the Boltzmann's factor shows that this behavior will exist no matter what values of the parameters are chosen, and simply represents the inadequacy of our model in the high-temperature region.

V. Conclusion

Using a simple phenomenological model with a mixed parametrization from extended Hückel and LAPW methods, we were able to investigate the temperature-dependent concentration of charge carriers in a low-dimensional infinite system. We found that this model was able to describe the thermal behavior of metallic conductivity, within a given range of temperature, if one makes the assumption that the number of charge carriers can be directly related to electrical conductivity. One major point is that this approach relies on band structure calculations. Therefore, we were able to explicitly take into consideration electronic and geometric factors which were not reflected in former studies. Despite its approximate framework, it made it possible to give some new insights into transport phenomena in metals. Specifically it provided an intuitive feel for what is meant by electron−phonon scattering. Following Peierls's theorem, we focused on the ω_o − mode. However, the participation of the whole phonon spectrum could be traced with, presumably, little additional information. As far as the dimensionality of the system is concerned, one might expect some interesting variations since in two and three dimensions the density of states expands as k^2 and k^3, respectively. However our main result, that the number of charge carriers in metallic systems can be reduced through vibronic interaction, will be unchanged. The influence of external fields as well as the effect of electronegativity alternation along the chain should also be studied using a similar approach. We intend to explicitly take into account the role of overlap in the band structure description. The effective modulation of vibronic constant with overlap is left for future publication.

Acknowledgment. The authors thank Professors R. S. Berry and T. R. Hughbanks for helpful discussions.

Appendix

The FLAPW calculations were performed with the Moruzzi, Janak, and Williams functional.[19] RK_{max} was set equal to 6.0, and 10 radial functions were used inside the spheres of radius 2.1. The potential was expanded inside the spheres using spherical harmonics with $l \leq 4$, and 100/20 k-points within the cell/zone were used.

References and Notes

(1) Bersuker, I. B.; Polinger, V. Z. *Vibronic Interactions in Molecules and Crystals*; Spinger-Verlag: Berlin, 1989.

(2) Öpik, U; Pryce, M. H. L. *Proc. R. Soc. London, Ser. A.* **1957**, *238*, 425.

(3) Jahn, H. A.; Teller, E. *Proc. Roy. Soc. A* **1937**, *161*, 220.

(4) Piepho, S. B.; Krausz, E. R.; Schatz, P. N. *J. Am. Chem. Soc.* **1978**, *100*, 2996.
(5) Piepho, S. B. *J. Am. Chem. Soc.* **1988**, *110*, 6319.
(6) Piepho, S. B. *J. Am. Chem. Soc.* **1990**, *112*, 4197.
(7) Fischer, F.; Köppel, H.; Cederbaum, L. S. *Il Nuovo Cimento* **1987**, *9d*, 571.
(8) Holstein, T. *Ann. Phys. (New York)* **1959**, *8*, 325.
(9) (a) Su, W.-P.; Schrieffer, J. R.; Heeger, A. J. *J. Phys. Rev. Lett.* **1979**, *42*, 1698. (b) Su, W.-P.; Schrieffer, J. R.; Heeger, A. J. *Phys. Rev. B* **1980**, *22*, 2099. (c) Heeger, A. J.; Kivelson, S.; Schrieffer, J. R.; Su, W.-P. *Rev. Mod. Phys.* **1988**, *60*, 781.
(10) De Gennes, P.-G. *Phys. Rev.* **1960**, *1*, 141.
(11) Kittel, C. *Introduction to Solid State Physics*; Wiley: New York, 1986.
(12) Dufek, P.; Blaha, P.; Sliwko, V.; Schwarz, K. *Phys. Rev.* **1994**, *B49*, 10170.
(13) Blaha, P.; Schwarz, K.; Dufek, P.; Augustyn, R. *WIEN95*; Technical University of Vienna, 1995. (Improved and updated Unix version of the original copyrighted WIEN-code, see: Blaha, P.; Schwartz, K.; Sorantin, P.; Trickey, S. B. *Comput. Phys. Commun.* **1990**, *59*, 399).
(14) Albright, T. A.; Burdett, J. K.; Whangbo, M.-H. *Orbital Interactions in Chemistry*; Wiley: New York, 1985.
(15) Peierls, R. *Quantum Theory of Solids*; Clarendon: Oxford, U.K., 1955.
(16) (a) Burdett, J. K. *Prog. Sol. State Chem.* **1984**, *15*, 173. (b) Hoffmann, R. *Solids and Surface: A Chemist's View of Bonding in Extended Structures*; VCH: New York, 1988.
(17) Cohen-Tannoudji, C.; Diu, B.; Laloë, F. *Mécanique Quantique*; Hermann: Paris, 1992.
(18) Anderson, A. B.; Hoffmann, R. *J. Chem. Phys.* **1974**, *60*, 4271.
(19) Moruzzi, V. L.; Janik, J. F.; Williams, A. R. *Calculated Properties of Metals*; Pergamon: New York, 1978.